

*Effects of Ag doping amount on structural properties of zinc oxide  
nanostructures*

Kyung Ho Kim<sup>\*</sup>, Daisuke Mamiya, Yoshio Abe, Midori Kawamura

Department of Materials Science and Engineering, Kitami Institute of Technology,  
165 Koen-cho, Kitami, Hokkaido 090-8507, Japan

**Abstract**

We investigated the structural properties of zinc oxide (ZnO) nanostructures grown on the glass substrates using the chemical solution deposition while being doped with Ag in different amounts. The undoped ZnO nanostructures were composed of flower-like bundles consisting of nanorods with a length of  $\sim 2.3 \mu\text{m}$  and hexagonal disks with a diameter of  $\sim 2.2 \mu\text{m}$  and thickness of  $\sim 350 \text{ nm}$ . In these flower-like bundles, the diameter and density of the nanorods at the center were smaller and higher, respectively, than those of the nanorods at the edge. With addition of Ag in the ZnO, the Ag nanoparticles were formed on the substrate, which led to suppress the growth of the flower-like bundles and decrease the thickness of the disks. The intensities of the

diffraction peaks corresponding to the ZnO and Ag phases decreased and increased, respectively, with an increase in the amount of Ag added. It was found that the Ag-doped ZnO nanostructures contained Ag particles, which formed a continuous thin film, resulting in low sheet resistance ( $\sim 1 \Omega/\text{sq}$ ).

**Keywords:** ZnO; Ag; Flower-like bundles; Nanorods; Disks

**Corresponding author:** Kyung Ho Kim, Tel: 81-157-26-9431, Fax: 81-157-26-4973,

E-mail: [khkim@mail.kitami-it.ac.jp](mailto:khkim@mail.kitami-it.ac.jp)

## 1. Introduction

Recently, zinc oxide (ZnO) nanostructures have received significant attention owing to their outstanding potential for use in various nano-scaled electronic and optoelectronic devices [1-5]. It was reported that the nanodisk ZnO exhibited excellent gas-sensing performances by Zhao *et al.* [6]. Tang and coworkers reported outstanding photoluminescence properties of the nanoflower-shaped ZnO [7,8]

In our previous study, we had investigated the properties of Li-doped and Cu-doped ZnO nanorods and had compared them to those of undoped ZnO nanorods grown on ZnO seed layers formed on fluorine-doped tin oxide (FTO)-coated glass substrates [9]. When ZnO was doped with Li, long and well-aligned nanorods could be grown. On the other hand, the use of Cu as a dopant triggered a morphological change in the ZnO. Under the same growth conditions, the addition of dopants resulted in the synthesized ZnO nanorods exhibiting a different growth behavior [9-11]. In addition, we found that the substrate materials used also played an important role in determining the characteristics of the grown ZnO nanorods [12]. When compared to the ZnO nanorods grown on FTO and silicon substrates, those grown on glass substrates exhibited poorer crystal quality, owing to the poor adhesion between the nanorods and the glass substrates.

In this study, we investigated the effects of the Ag doping amount on the structural properties of ZnO nanostructures grown on glass substrates using a solution deposition method.

## 2. Experimental

The ZnO seed layer was prepared using an aqueous solution of zinc acetate dihydrate ( $\text{Zn}(\text{CH}_3\text{COO})_2 \cdot 2\text{H}_2\text{O}$ , 0.25 M). 20  $\mu\text{L}$  of the solution was dropped on a glass substrate (Eagle XG,  $2 \times 2 \text{ cm}^2$ ) and spin-coated at a speed of 2000 rpm for 30 s. It was then dried at 250 °C for 5 min and subsequently annealed at 350 °C for 30 min in air.

The ZnO nanostructures were fabricated by the chemical solution deposition using an aqueous solution of zinc nitrate hexahydrate ( $\text{Zn}(\text{NO}_3)_2 \cdot 6\text{H}_2\text{O}$ , 0.01 M) and HMT ( $\text{C}_6\text{H}_{12}\text{N}_4$ , 0.01 M). The pH value of the solution was 7.1. To grow Ag-doped ZnO (AZO) nanostructures, silver nitrate was added to the above-mentioned solution in different amounts: 0.1 mM (pH 7.0, labeled as AZO1), 0.5 mM (pH 7.0, labeled as AZO2), and 3 mM (pH 6.9, labeled as AZO3). The substrates with the ZnO seed layers were immersed vertically in the aqueous solution at 90 °C for 6 h. The samples were then washed with deionized water and dried at 120 °C for 10 min.

The crystal structures and orientations of the various ZnO nanostructures were

observed using X-ray diffraction (XRD, Bruker, D8ADVANCE) analyses. Their surface morphologies were examined using a field emission scanning electron microscopy (FESEM, JSM-6701F) system to which an energy dispersive X-ray spectrometry (EDX) detector was attached. The electrical property of the ZnO nanostructures was characterized using a four-point probe.

### **3. Results and discussion**

Figure 1 shows the XRD pattern of undoped ZnO nanostructures grown on a glass substrate. The diffraction peaks at  $31.7^\circ$ ,  $34.4^\circ$ , and  $36.2^\circ$  correspond to the (100), (002), and (101) planes, confirming that the ZnO is the hexagonal wurtzite structure (JCPDS card no. 36-1451) (see Table S1 in the supporting information).

Figure 2(a,b) show the top-view and cross-sectional FESEM images of the undoped ZnO nanostructures. It can be seen from the top-view image (Fig.2(a)) that the nanostructures consisted of flower-like bundles of nanorods and hexagonal disks were distributed randomly on the surface of the glass substrate. Further, it can be seen from the cross-sectional image (Fig.2(b)) that the nanorods with a length of  $\sim 2.3 \mu\text{m}$  grew radially on the surface of the substrate and formed a semicircle. It is worth noting that there were no apparent cracks or detachments between the nanostructures and the glass

substrate. Figures 2(c) and (d) are the high-magnification images of the areas at the center and edge region, respectively, marked in Fig.2(a) by dotted squares. The hexagonal nanorods at the center of the flower-like bundle had a diameter of  $140 \pm 20$  nm and a density of  $\sim 33 \mu\text{m}^{-2}$ ; these values are lower and higher, respectively, than those of the nanorods at the edge region. These characteristics of the flower-like bundles formed by the assembly of nanorods are similar to those reported by Hu *et. al.* [13]. Finally, it can be seen from Fig.2(e) that the disk had a diameter of  $\sim 2.2 \mu\text{m}$  and thickness of  $\sim 350$  nm.

The presence of elemental O, Zn, and Pt in the undoped ZnO nanostructures could be confirmed from EDX spectrum, as shown in Fig.3. The appearance of the Pt-related peaks in the spectrum was attributable to the Pt coating. The fact that only elemental O and Zn were detected confirmed that the fabricated ZnO nanostructures were highly pure.

Figure 4 (a-c) show top-view images of the AZO nanostructures formed by doping ZnO with Ag in various amounts. AZO1, which was formed by the incorporation of 0.1 mM Ag in ZnO (Fig.4(a)), consisted of flower-like bundles formed by the assembly of nanorods and hexagonal disks. Compared to the density of the nanorods in the flower-like bundles of the undoped ZnO nanostructures (Fig.2(a)), that of the nanorods

in the AZO nanostructures was relatively low. With an increase in the Ag doping amount to 0.5 mM (Fig.4(b)), particles with a diameter of  $\sim 200$  nm grew randomly on the surface of the substrate. It can be seen from the top-view image of the AZO3 sample (see Fig.4(c)) that nanorods with a length of  $\sim 2.2$   $\mu\text{m}$  (indicated by arrows) grew in distributed manner and flower-like bundles were not formed. The diameter of the particles increased to  $\sim 900$  nm with an increase in Ag doping amount to 3 mM. Further, thickness of the nanoparticles on the glass substrate was  $\sim 600$  nm, as shown in cross-sectional FESEM image of AZO3 (Fig.4(d)). Interestingly, the length of the nanorods and the diameter of the disks were less sensitive to the Ag doping amount. Meanwhile, as shown in Fig.4(e), the thickness of the disks in the case of AZO3 decreased to  $\sim 70$  nm, with nanoparticles with a diameter of  $\sim 30$  nm clinging to the surface of the disks. The whole surface of the AZO3 sample is white to the naked eye.

Figure 5 shows the XRD patterns of the AZO nanostructures grown using different Ag doping amounts. All samples exhibited diffraction peaks corresponding to ZnO at  $31.7^\circ$ ,  $34.4^\circ$ , and  $36.2^\circ$  (denoted by circles); these were attributable to the (100), (002), and (101) planes, respectively (see Table S1). There is no distinguished peak shift with increasing Ag amounts in the ZnO. The intensities of the ZnO peaks decreased with the incorporation of Ag (Fig.2(a)), becoming lower than those in the case of the undoped

ZnO (Fig.1). It would be due to lower density of the nanorods in the bundles of the ZnO nanostructure with incorporation of the Ag. As can be seen from Figs.5(b,c), XRD peak was observed at  $38.0^\circ$  (marked by a square) corresponding to the (111) plane of the face-centered cubic Ag structure (JCPDS card no. 04-0783); it confirmed that the particles in the AZO2 and AZO3 samples were metallic silver and no silver oxide phase was present in the samples. It was because Ag might diffuse out of the ZnO lattice due to the limit of the solubility and form a metallic Ag phase [14,15]. The Ag particles that grew on the surface of the substrate may be attributed to the suppression of the formation of the flower-like bundles, which eventually resulted in the growth of individually distributed nanorods instead in the AZO3. When compared to the intensity of the peak corresponding to the Ag (111) plane in case of AZO2, that of the peak of the case of AZO3 was significant higher. The AZO3 had low sheet resistance ( $\sim 1 \Omega/\text{sq}$ ).

#### **4. Conclusions**

We grew ZnO nanostructures on the glass substrates under simple growth conditions and investigated their structural properties, compared them to those of AZO nanostructures. The ZnO nanostructures consisted of flower-like bundles formed by the assembly of nanorods, which grew radially on the surface of the substrate. Further,

hexagonal disks also grew randomly on the substrate. The amount of Ag doped in ZnO had a significant effect on the growth of the flower-like bundles and hexagonal disks. With an increase in the doping amount to 3 mM, Ag particles grew uniformly on the substrate surface, forming a thin film. In addition, it was found that the AZO3 nanostructures exhibited low sheet resistance.

## Figure captions

Fig.1. XRD pattern of the ZnO nanostructures grown on the glass substrate.

Fig.2. FESEM images of the ZnO nanostructures; (a) top-view image, (b) cross-sectional image, (c,d) high-magnification images of the areas marked by dotted squares at center and edge regions in (a), and (e) high-magnification image of a hexagonal disk.

Fig.3. EDX spectrum of the ZnO nanostructures.

Fig.4. FESEM images of the AZO nanostructures; (a-c) top-view images of AZO1, AZO2, and AZO3, (d) cross-sectional image of AZO3, (e) high-magnification image of the area marked by a dotted square in (c).

Fig.5. XRD patterns of the AZO nanostructures formed using different Ag doping amounts; (a) 0.1 mM (AZO1), (b) 0.5 mM (AZO2), and (c) 3 mM (AZO3).

## References

- [1] S. Kar, B.N. Pal, S. Chaudhuri, D. Chakravorty, *J. Phys. Chem. B* 110 (2006) 4605-4611.
- [2] A. Umar, M.M. Rahman, S.H. Kim, Y-B. Hahn, *Chem. Commun.* (2008) 166-168.
- [3] Y-S. Choi, J-W. Kang, D-K. Hwang, S-J. Park, *IEEE Trans. Electron Devices* 57 (2009) 26-41.
- [4] K. Park, D-K. Lee, B-S. Kim, H. Jeon, N-E. Lee, D. Whang, H-J. Lee, Y.J. Kim, J-H. Ahn, *Adv. Funct. Mater.* 20 (2010) 3577-3582.
- [5] R. Tao, T. Tomita, R.A. Wong, K. Waki, *J. Power Sources* 214 (2012) 159-165.
- [6] Q. Zhao, Q. Shen, F. Yang, H. Zhao, B. Liu, Q. Liang, A. Wei, H. Yang, S. Liu, *Sens. Actuators B* 195 (214) 71-79.
- [7] L. Hongjin, Z. Zang, X. Tang, *Opt. Mater. Express* 4 (2014) 1762-1769.
- [8] Z. Zang, X. Tang, *J. Alloys Compd.* 619 (2015) 98-101.
- [9] K.H. Kim, Z. Jin, Y. Abe, M. Kawamura, *Superlattice. Microst.* 77 (2015) 101-107.
- [10] S.H. Chiu, J.C.A. Huang, *J. Non-Cryst. Solids* 358 (2012) 2453-2457.
- [11] Y. Caglar, A. Arslan, S. Ilican, E. Hür, S. Aksoy, M. Caglar, *J. Alloys Compd.* 574 (2013) 104-111.
- [12] K.H. Kim, K. Utashiro, Y. Abe, M. Kawamura, *Int. J. Electrochem. Sci.* 9 (2014)

2080-2089.

[13] X. Hu, Y. Masuda, T. Ohji, K. Kato, *Appl. Surf. Sci.* 255 (2008) 2329-2332.

[14] T. Ivanova, A. Harizanova, T. Koutzarova, B. Vertruyen, *Superlattice. Microst.* 70 (2014) 1-6.

[15] A. Meng, S. Sun, Z. Li, J. Han, *Adv. Powder Technol.* 24 (2013) 224-228.

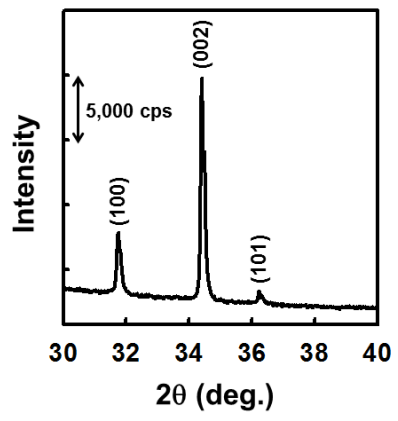


**Fig. 1.**

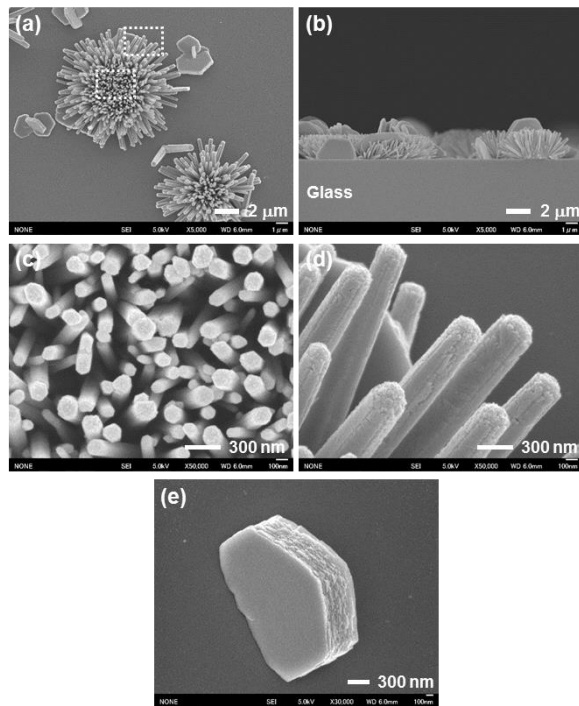


**Fig. 2.**

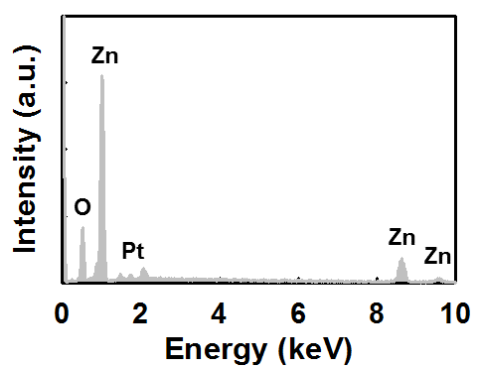


**Fig. 3.**

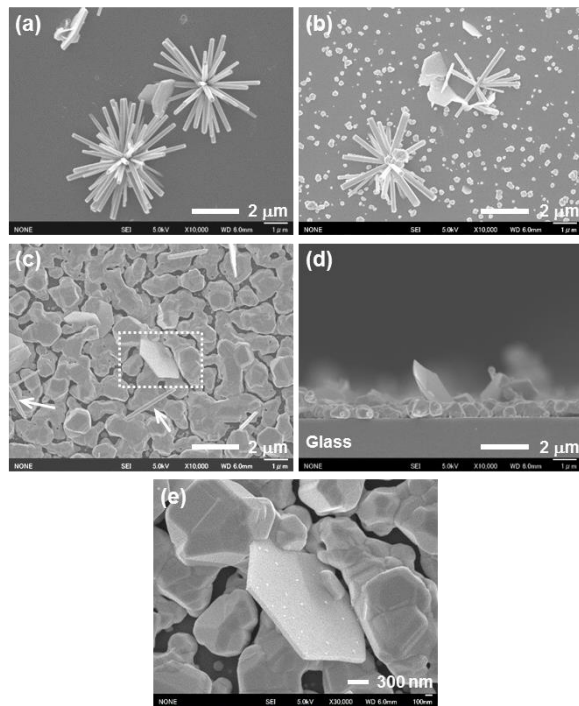


**Fig. 4**

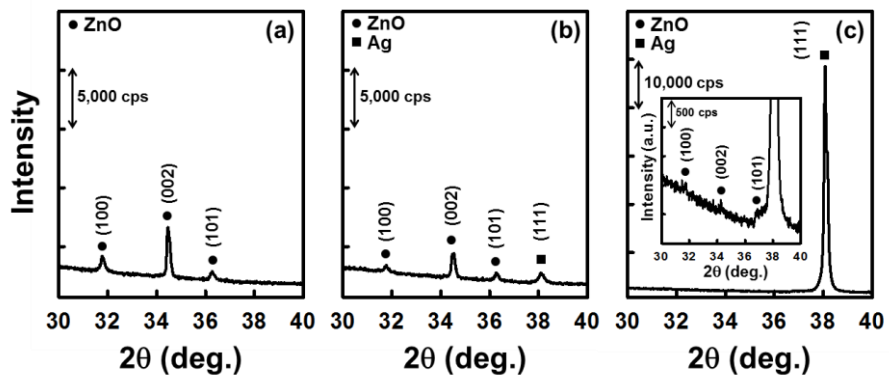


Fig. 5.